SHO Filter Comparison Test

by Jim Thompson, P.Eng
Test Report – August 23rd, 2022

Introduction:
Over the years I have dedicated a lot of time to characterizing the performance of astronomical filters. I have done so primarily from the standpoint of an astro-dedicated camera user, but I do not consider myself to be an astrophotographer. My application of cameras has been for Electronically Assisted Astronomy (EAA), using a camera to enhance the observing experience. That said, many of the requirements for an effective EAA filter apply to astrophotography as well, and visa versa. That is why I have recently spent some time looking at Sulfur-Hydrogen-Oxygen or SHO narrowband filter sets. My interest in the topic was triggered when I received a sample set of the Optolong 3nm SHO filters to try out. I already owned an IDAS 6.8nm Hα and 6.5nm O-III filter, so this seemed like a good opportunity to perform another comparison test. Thus, the purpose of this test report is to evaluate two SHO filter sets of different bandwidths, and compare their performance.

Objective:
The objective of this test report is to evaluate the performance of two SHO filter sets, one in the 6.0 to 7.0nm band width range, and the other in the 3.0nm band width range. Use of the term bandwidth in this report refers specifically to the filter's full width half maximum (FWHM), the wavelength range over which the filter's transmissivity is more than 50% of it's maximum. The list of filters used in this test report is as follows (costs are for 2" version):

- No Filter (for reference)
- Set #1: IDAS H-α 6.8nm *($379USD*), IDAS O-III 6.5nm (*$379USD*), Optolong S-II 6.5nm (*$250USD*) – Total Set Cost $929USD
- Set #2: Optolong H-α 3nm (*$439USD*), Optolong O-III 3nm, Optolong S-II 3nm – Total Set Cost $1249USD (on sale presently $991USD)

Some of the filters are available individually, the price for which is noted in italics above. IDAS does not currently sell an S-II narrowband filter, so for this test I rounded out the IDAS set with an Optolong 6.5nm S-II filter I found for sale used online. If theory is born out in the test results, there should be an observable improvement in deepsky object contrast moving from Set #1 to #2 since it has narrower pass bands. Filter performance is evaluated during this test based on the increase in contrast between the observed object and the background, which is a measurable quantity. It was evaluated quantitatively using the measured filter spectra combined with the spectra of several common deepsky objects, and by direct measurement from images captured using each filter and a monochrome camera. The image data is also used to evaluate the signal-to-noise ratio (SNR) achieved using each filter.

Method:
Testing consisted of data collection from the following sources:

- Spectral transmissivity data, from near-UV to near-IR, measured using an Ocean Optics USB4000 spectrometer; and

- Image data, collected using a Mallincam Skyraider DS432M-TEC monochrome camera, and one of three different refractors:
    - William Optics Zenithstar 80 II ED;
    - William Optics FLT98 triplet apochromatic; or
    - Askar FMA230 quad apochromatic.

The spectrometer data was collected in my basement workshop with the USB4000 and a broad spectrum light source. Filter spectrums were measured for a range of filter angles relative to the light path, from 0° (perpendicular) to 20° off-axis. The spectrometer was recently upgraded, replacing the entrance slit and diffraction grating, to give a wavelength resolution of 0.5nm.

The image data was collected from one of two locations: my backyard in central Ottawa, Canada where the naked eye limiting magnitude (NELM) due to light pollution is +2.9 on average (Bortle 9+); and at my cottage near Petawawa, Canada where the skies are Bortle 5. I switched filter configurations using a ZWO 2" filter drawer. Each time I changed filters I refocused on a conveniently located bright star using a Bahtinov mask. Images with the various filters under test were collected with the scopes at their native focal ratios: f/6.8 for the ZS80, f/6.3 for the FLT98, and f/4.5 for the FMA230. Images of three different deepsky object were captured, each on a different evening as follows:

1. M8 Lagoon Nebula, July 8th, using ZS80, at cottage
2. IC1318 Oriental Dragon Nebula, August 2nd, using FMA230, at home
3. NGC6960 Western Veil Nebula, August 12th, using FLT98, at home

The purpose of selecting different deepsky objects was to use the filters on targets with varying amounts of H-α, O-III and S-II emission. The Moon had an impact on the first imaging night, it being 5 days before the full Moon. The Moon was set at the time of the second imaging session. The third imaging session was on the night after the full Moon, so the Moon had an impact on that data set as well.

Results – Spectrum Measurements:
Using the test method mentioned above the spectral transmissivity for each filter was measured for a range of filter angles relative to the light path. Figure 1 presents a plot of the resulting spectral transmissivity data for the case of the filter perpendicular to the light path. All the 6-7nm wide filters, plus the 3nm H-α filter, have their center wavelengths (CWL) well positioned over their respective emission bands. The 3nm O-III and S-II filters have their CWLs shifted to the left of their respective emission bands by approximately 1.5 to 2.0nm. Having the filter CWL shifted down in wavelength (to the left) is not optimum and will result in a detrimental impact on filter performance.

The impact of angle on each filter's respective emission band transmission is shown in Figure 2. As expected, filters with wider pass bands were less sensitive to angle than filters with narrow pass bands, with the most sensitive filters to angle being the 3nm samples. The 3nm O-III and S-II filters are particularly sensitive to angle due to their pass bands being shifted to the left as discussed above.

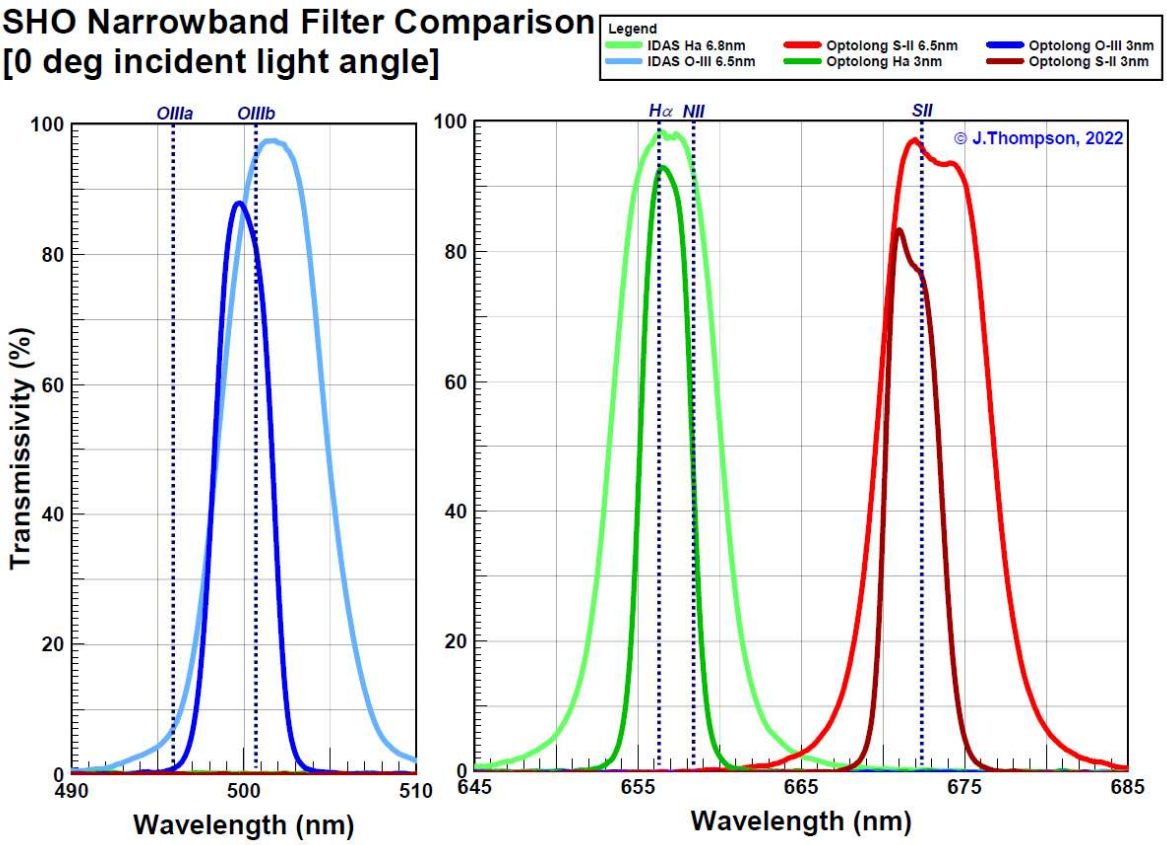

Figure 1 Measured Spectral Response of Tested Filters – Filter Perpendicular to Light Path

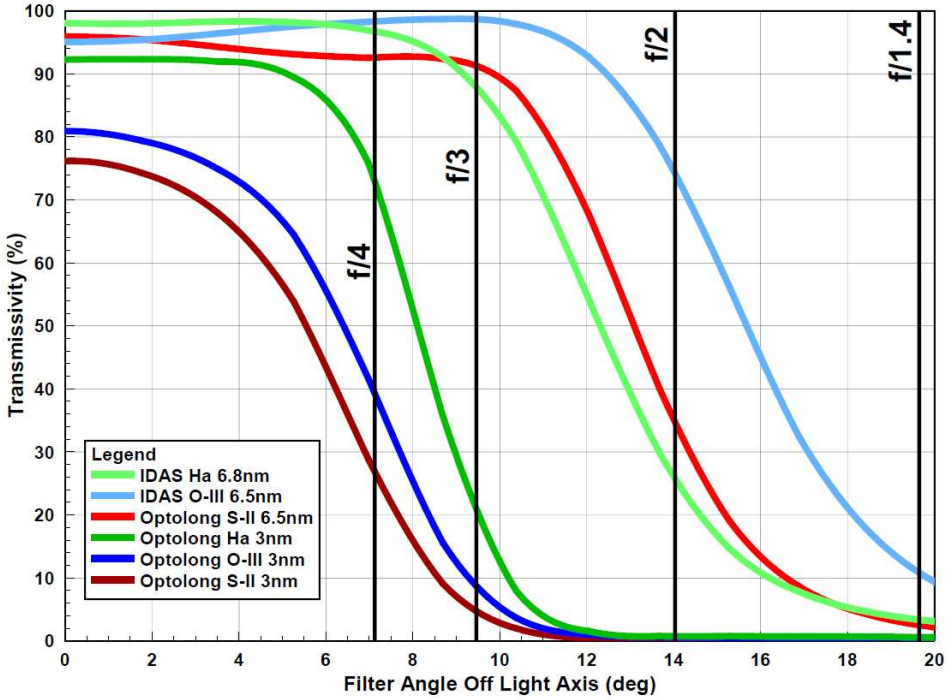

Figure 2 Measured Impact of Angle on Filter Response

Figure 2 also has black vertical lines representing different optics f-ratios. These lines are positioned at the angle values corresponding to light coming from the outer edge of the scope's aperture for the noted f-ratio. For example: for an f/2 scope the light from the outer edge of the optics is passing through the filter at a 14° angle. The net performance of a filter on any particular speed of optics is an area weighted average of the filter's performance, from the center of the optics (perpendicular light path) out to the edge of the aperture (max light path angle). Using the measured filter spectra at each angle I have calculated a net filter spectrum for a selection of telescope f-ratios. The area averaging process is illustrated in Figure 3. Essentially the aperture of the scope is divided into rings defined by the angles at which I have measured filter data. The percentage each ring is of the total primary optical area is the weighting applied to that particular spectrum in the average. Figures 4 through 7 present the resulting net spectra for the different speeds of telescope. The shift in filter response between that shown in Figure 1 and for the f/6.3 telescope (Figure 4) is almost zero, but is very significant for the f/2 scope (Figure 7). The effects of filter band shift are worse on the Hyperstar scope due to the large central obstruction which results in a larger percentage of the light having to pass through the filter at an angle.

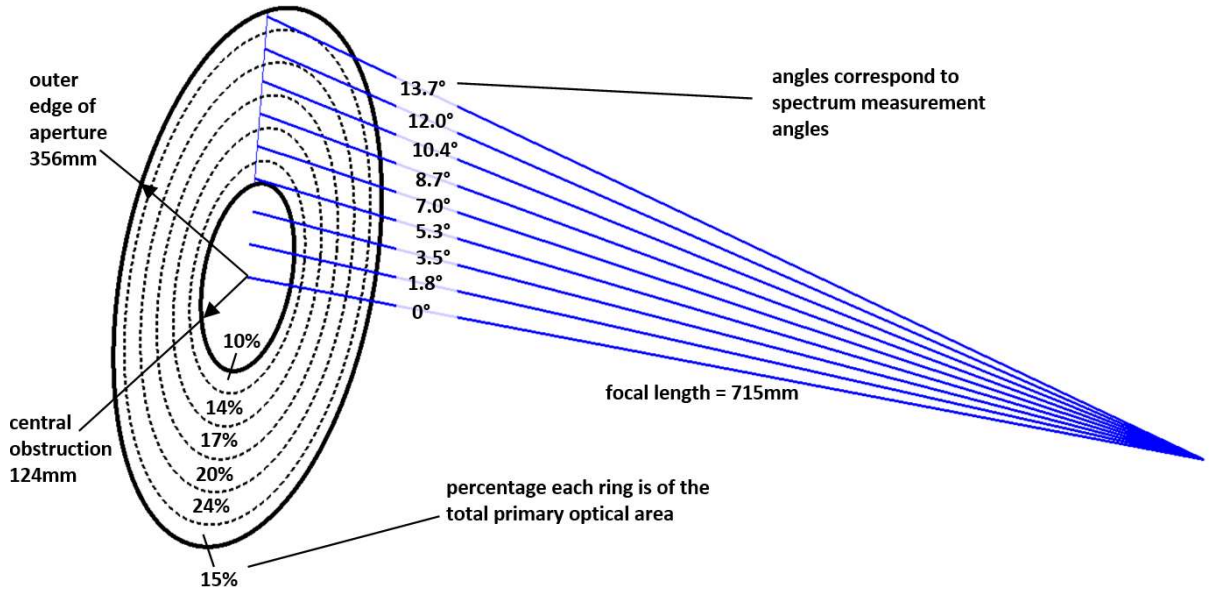

Figure 3 Illustration of Area Weighted Average Filter Response Calculation – C14 Hyperstar

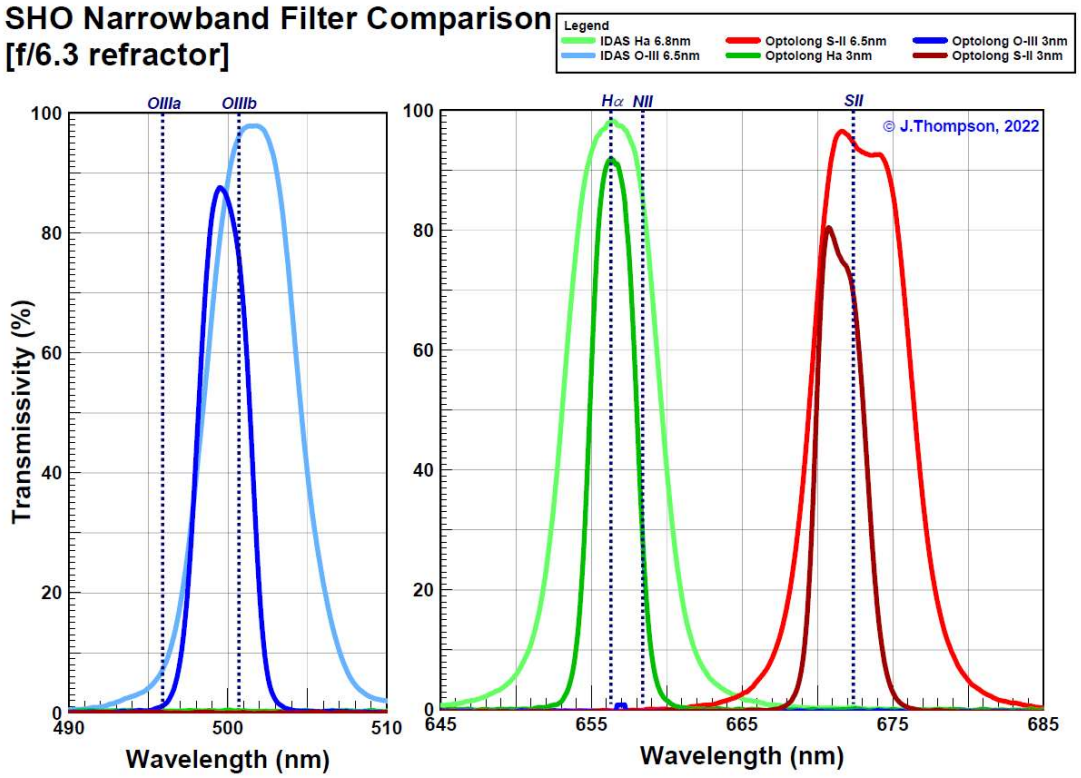

Figure 4 Net Spectral Response of Tested Filters – f/6.3 Refractor Area Weighted Average

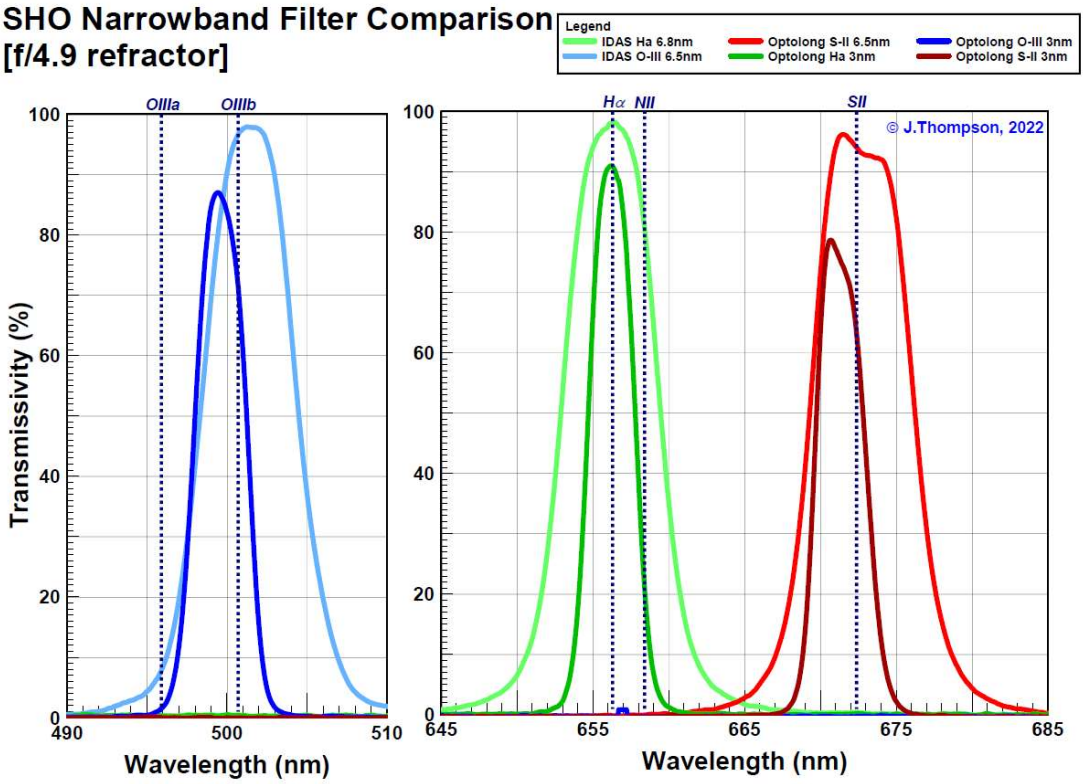

Figure 5 Net Spectral Response of Tested Filters – f/4.9 Refractor Area Weighted Average

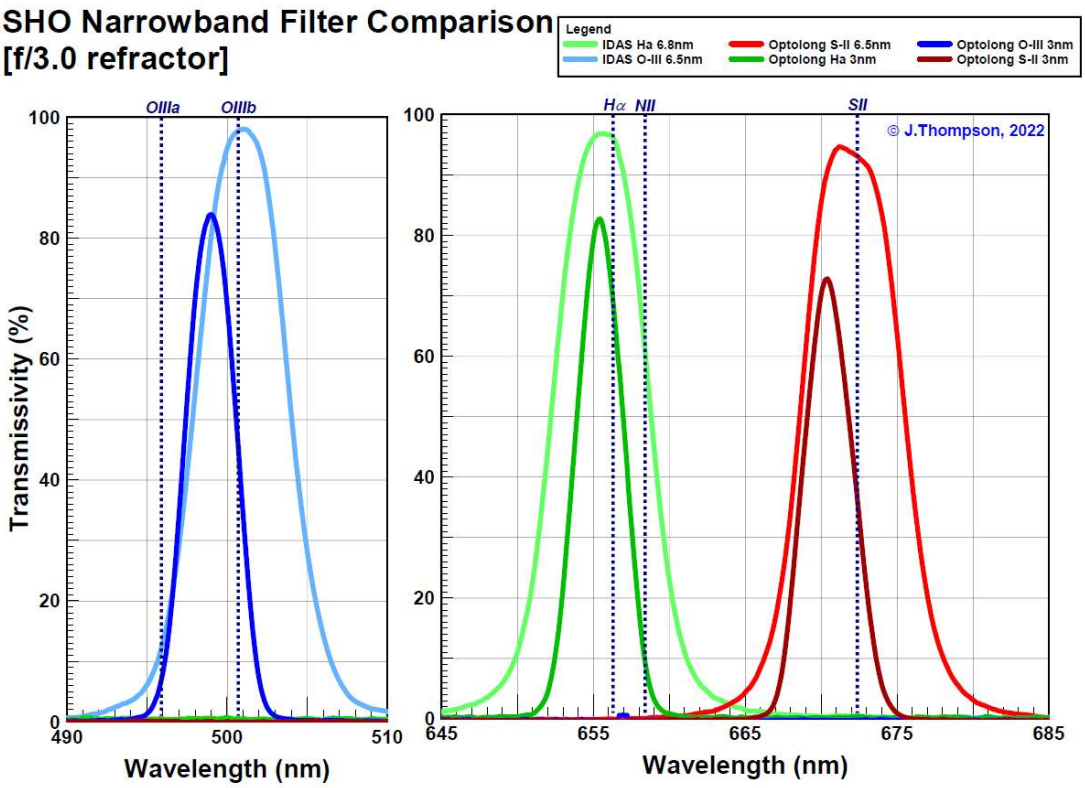

Figure 6 Net Spectral Response of Tested Filters – f/3.0 Refractor Area Weighted Average

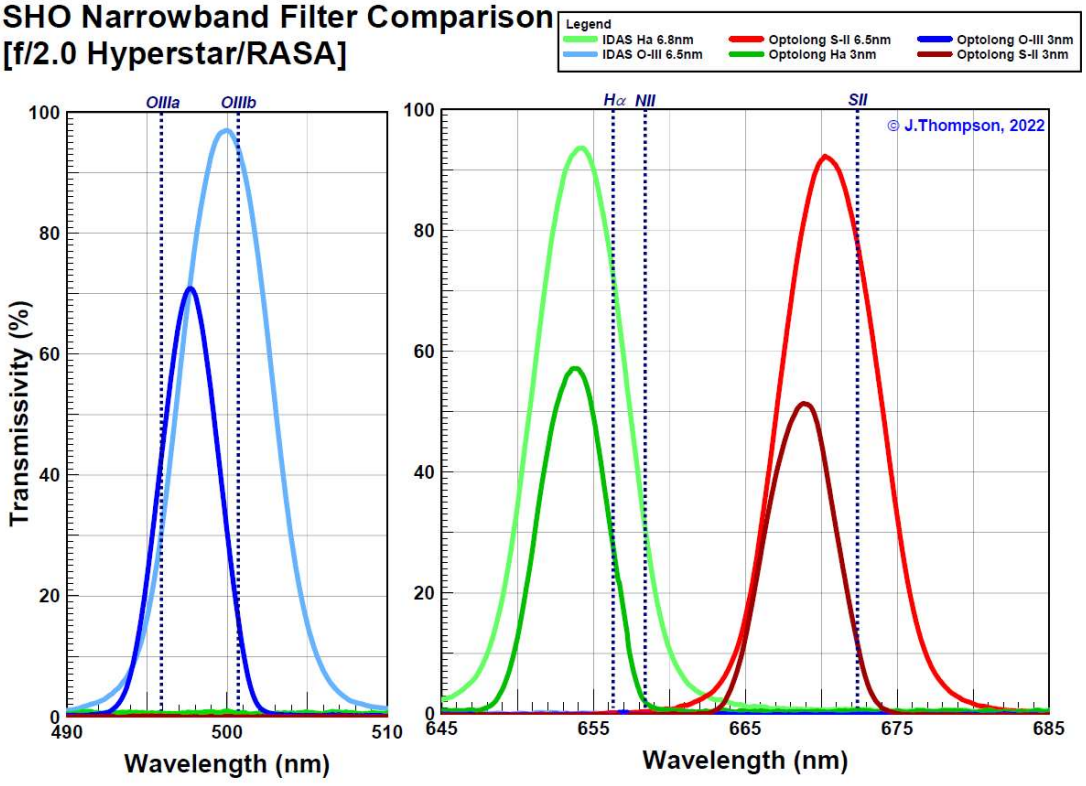

Figure 7 Net Spectral Response of Tested Filters – f/2 C14 w/Hyperstar Area Weighted Average

With the net filter spectra in hand, it is possible to extract overall performance related statistics for each filter, such as transmission values at key wavelengths of interest and pass band widths. These filter statistics are provided in Table 1, including a calculated value for percent Luminous Transmissivity (%LT), a single number that describes generally how much light is getting through the filter. The calculated value of %LT depends on the spectral response of the detector, which in this case is assumed to be a modern back illuminated monochrome CMOS sensor. I have included transmission measurements in the table for a range of telescope f-ratios, from f/∞ (perfectly parallel & perpendicular light) down to f/2.

Filter	Scope Optics	%LT*	FWHM	Transmissivity					
				Hbeta (486.1)	O-IIIa (495.9)	O-IIIb (500.7)	Halpha (656.3)	N-II (658.4)	S-II (672.4)
IDAS O-III 6.5nm	f/∞	1.72	6.3nm	0.2%	6.9%	95.0%	0%	0%	0%
	f/6.3**	1.67		0.4%	7.0%	96.1%	0%	0%	0%
	f/4.9**	1.66		0.4%	7.7%	96.7%	0%	0%	0%
	f/3.0**	1.66		0.4%	11.9%	97.8%	0%	0%	0%
	f/2***	1.67		0.5%	30.1%	93.9%	0%	0%	0%
IDAS H-α 6.8nm	f/∞	1.49	6.7nm	0%	0%	0%	98.0%	91.9%	0%
	f/6.3	1.43		0%	0%	0%	98.2%	85.3%	0%
	f/4.9	1.43		0%	0%	0%	98.1%	80.9%	0%
	f/3.0	1.43		0%	0%	0%	96.1%	61.1%	0%
	f/2	1.44		0%	0%	0%	72.6%	30.9%	0%
Optolong S-II 6.5nm	f/∞	1.46	7.1nm	0%	0%	0%	0%	0%	95.9%
	f/6.3	1.41		0%	0%	0%	0%	0%	94.6%
	f/4.9	1.40		0%	0%	0%	0%	0%	94.0%
	f/3.0	1.38		0%	0%	0%	0%	0.1%	93.1%
	f/2	1.38		0%	0%	0%	0.2%	0.4%	77.8%
Optolong O-III 3nm	f/∞	0.79	3.3nm	0%	0.9%	80.9%	0%	0%	0%
	f/6.3	0.77		0.1%	1.1%	75.8%	0%	0%	0%
	f/4.9	0.77		0.1%	1.5%	71.3%	0%	0%	0%
	f/3.0	0.77		0.1%	6.7%	45.4%	0%	0%	0%
	f/2	0.77		0.2%	42.5%	16.1%	0%	0%	0%
Optolong H-α 3nm	f/∞	0.64	3.1nm	0%	0%	0%	92.2%	45.8%	0%
	f/6.3	0.62		0%	0%	0%	91.9%	28.8%	0%
	f/4.9	0.63		0%	0%	0%	90.9%	21.4%	0%
	f/3.0	0.63		0%	0%	0%	69.3%	9.6%	0%
	f/2	0.64		0%	0%	0%	27.8%	2.0%	0%
Optolong S-II 3nm	f/∞	0.58	3.3nm	0%	0%	0%	0%	0%	76.2%
	f/6.3	0.55		0%	0%	0%	0%	0%	69.2%
	f/4.9	0.55		0%	0%	0%	0%	0%	63.2%
	f/3.0	0.54		0%	0%	0%	0%	0%	36.4%
	f/2	0.54		0%	0%	0%	0%	0%	11.6%

* calculated assuming spectral QE curve for IMX174M with no UV/IR blocking filter; ** refractor; *** C14 w/Hyperstar

Table 1 Measured Filter Performance Summary

Knowing the measured spectral response of the sample filters also allowed me to predict the theoretical relative performance of each filter when imaging an emission nebula. To do this I used the method I developed back in 2012 which applies the spectral response of the filter and sensor combined with the spectral emission from the deepsky object and background light polluted sky to estimate the apparent luminance observed. To help visualize the results of this analysis I have plotted the predicted % increase in contrast (vs. no filter) for each filter versus the filter's %LT. Figure 8 shows the resulting plot corresponding to filter performance when using a monochrome CMOS camera under moderately light polluted skies, Bortle 5 (i.e. same as at my

cottage). Note that these are theoretical predictions of the increase in visible contrast between the object and the background. The absolute values of my predictions may not reflect what a user will experience with their own setup, but the predicted relative performance of one filter to another should be representative. In general, the desired performance for a filter is high contrast increase and high %LT, so the higher and more to the right a filter's performance is in the plot the better. Each filter's performance is plotted as a short line to show how the performance is predicted to change depending on the f-ratio of the telescope you are using the filter with. Slow f-ratio optics are at the right-most end of the line, f/3 is roughly in the middle of the line, and f/2 is at the left-most end of the line. I have plotted predicted filter performance assuming the target is a typical emission nebula, Messier 8 the "Lagoon" nebula. I have selected this target for the performance predictions so that I can compare the numbers to my measurements which will be presented later in this report.

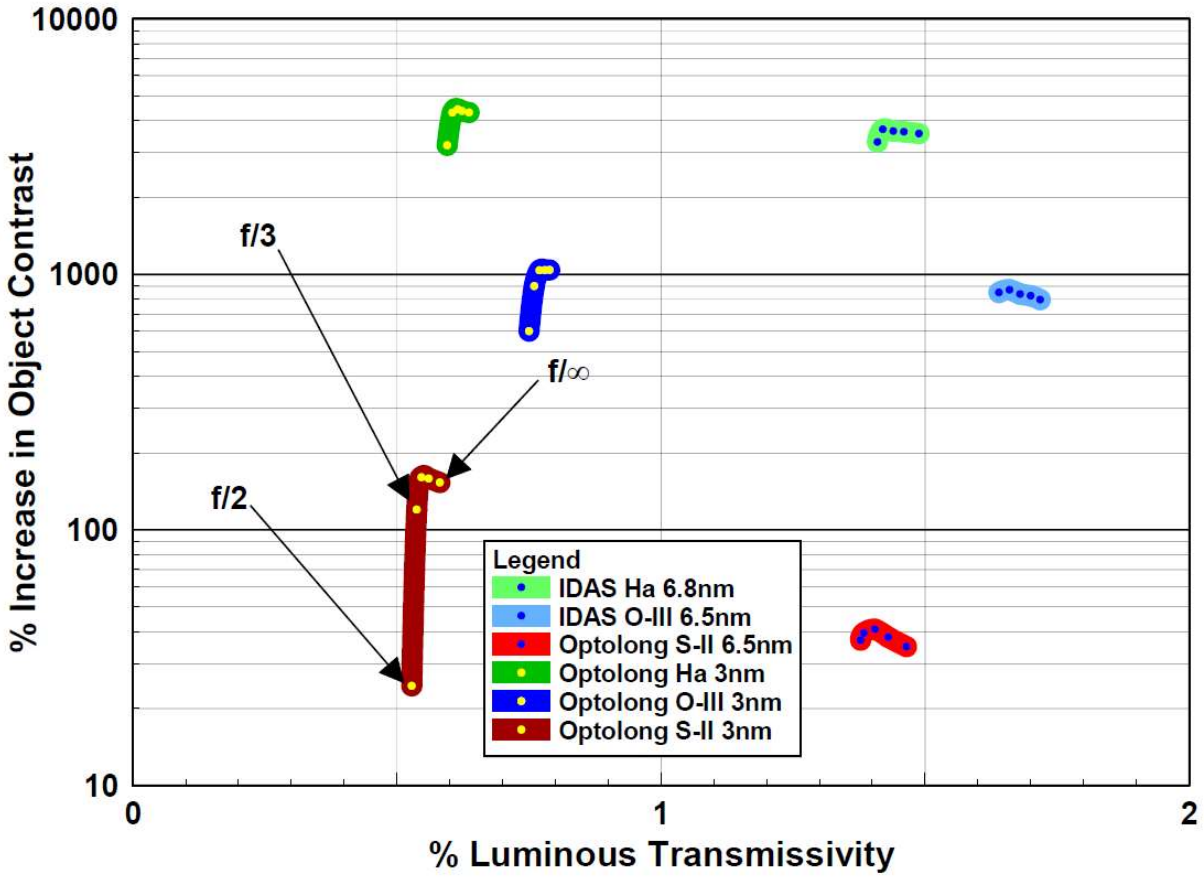

Figure 8 Predicted Filter Performance: M8, Back Illuminated Monochrome CMOS, Bortle 5 Sky

As expected, the predictions suggest that the narrower the filter's pass band (and thus lower %LT), the larger the contrast increase. The wider filters are predicted to deliver a consistent increase in contrast, one that does not change significantly down to an f-ratio of f/2. The three 3nm filters deliver a contrast increase that varies widely with f-ratio, but in general are predicted to always deliver higher performance than the other filters tested down to an f-ratio of f/3. The main drawback of the 3nm filters is that your exposure time will have to increase to compensate

for the lower %LT. This trade-off between contrast increase and exposure time is evident from Figure 8. For example: when used at f/6.3 the Optolong 3nm H-α filter is predicted to provide a contrast increase 1.2x that of the IDAS 6.8nm (4360% vs. 3616%), at the cost of 2.3x the exposure (%LT of 0.64% vs. 1.46%).

Results - Imaging:
All image collection on a particular night was done within a two-hour time window. This process was repeated three times, each on a different deepsky target as described above. The camera sub-exposures were saved to a folder and then stacked later using Deep Sky Stacker, generating a 16-bit FITS file. Sub-exposures captured using the 6-7nm filters were done at 30s each, and for the 3nm filters 45 to 50s each. A sufficient number of sub's were captured in each case to generate a stack with 10 minutes total exposure.

Imaging results from the three sessions are provided below in Figures 9 to 11. The images presented are of the final stacks. All the images had their histograms adjusted in exactly the same way using Fitswork v4.47, a free FITS editing software, so that they provide as fair a visual comparison as possible. To make the O-III and S-II images easier to visually compare, their histograms were stretched considerably more than for the H-α images. As a result the O-III and S-II images have also been passed through a noise reduction application to reduce the noise that resulted from the aggressive histogram stretch.

To be frank, I am not particularly happy with my imaging results. The signal strength of O-III and S-II in the objects I was trying to capture was very low relative to H-α. I should have been using much longer sub-exposure times instead of trying to stretch the histograms of my short sub-exposure images. To put it another way, nebulosity in the H-α images generally filled the bottom 14-bits of a possible 16 in the stacked images (luminance values 14,000 to 19,000), while nebulosity in the O-III images only used the bottom 12½-bits (luminance 5000 to 6000) and in the S-II images the bottom 11½-bits (luminance 2500 to 3000). Thus, the dynamic range of the camera was not being taken properly advantage of with my short sub-exposure times, especially for the O-III and S-II sub's.

Outside of the issue with exposure times, there are some general observations that can be made from the images. First, the 3nm H-α and S-II images appear to have better contrast than the 6-7nm wide filters. This is as expected based on the spectrometer results, although visually the differences are subtle. Second, the IDAS 6.5nm O-III images appear to have the same contrast as the Optolong 3nm O-III images. This is not the expected result based on what was observed in the spectrometer results. It is possible that the perceived differences could be more significant if longer sub-exposure times were used.

As I already mentioned earlier, I am not an astrophotographer. Nonetheless I have made an attempt to combine my individual band images into colour Hubble palette images. The results are presented in Figure 12. My images are rather clumsily put together but do provide another point of comparison between the 6-7nm filters and the 3nm filters. Generally, more faint detail is observable in the 3nm images, as well as fewer stars. Whether or not the same level of detail produced using the 3nm filters can be achieved with additional processing of the 6-7nm images is a question that is outside of my experience.

IDAS 6.5nm O-III (20 x 30s)

Optolong 3nm O-III (12 x 50s)

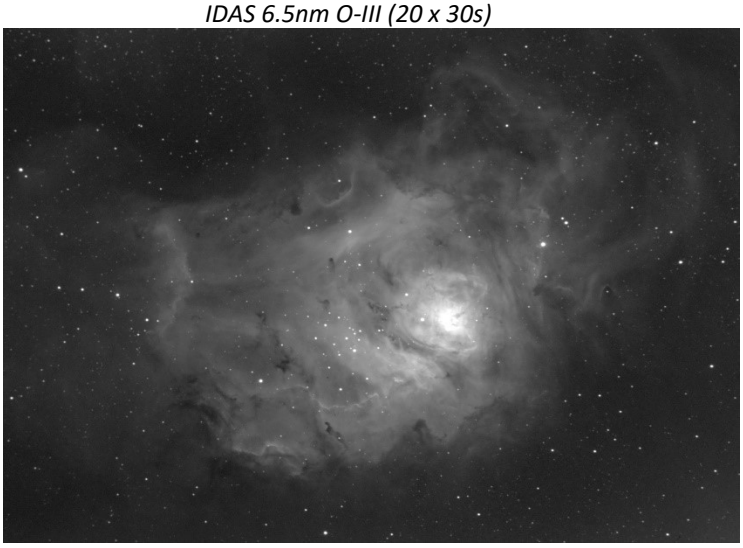

IDAS 6.8nm H-α (20x30s)

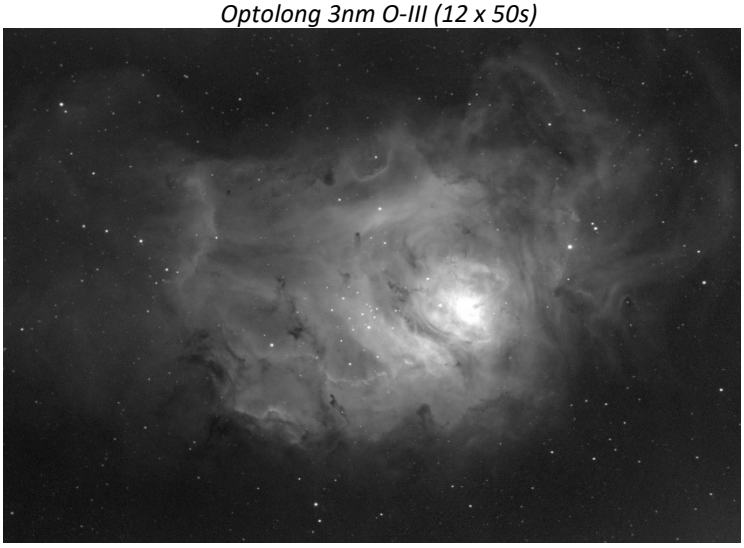

Optolong 3nm H-α (12 x 50s)

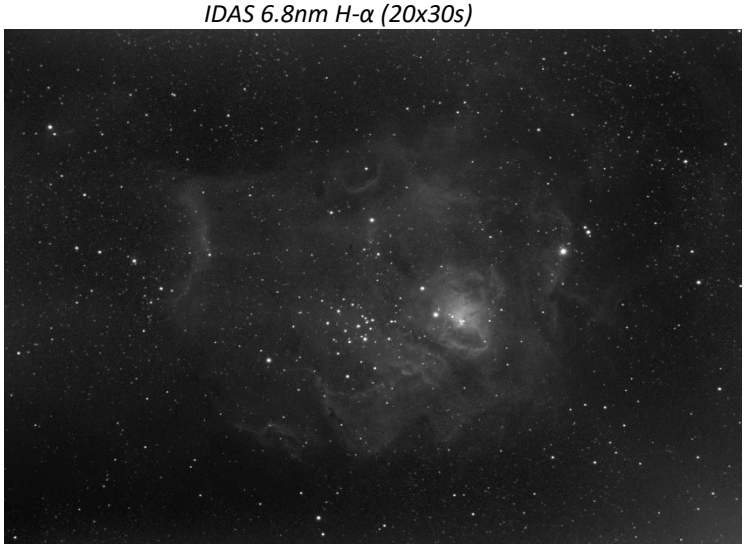

Optolong 6.5nm S-II (20 x 30s)

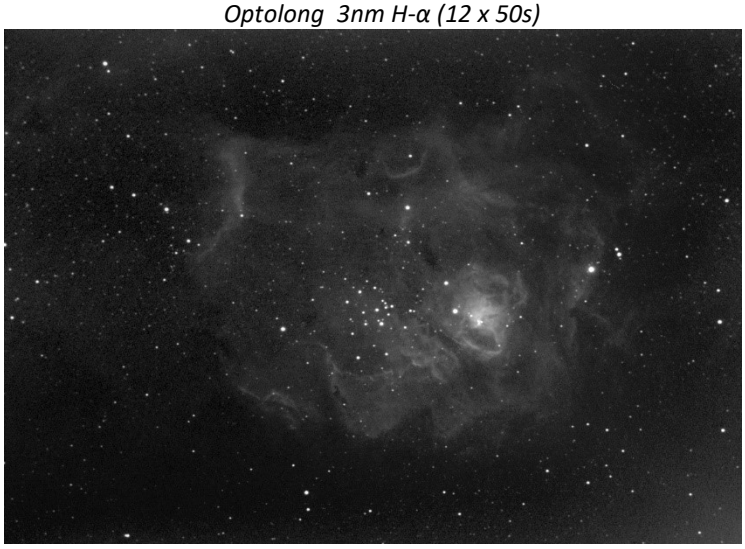

Optolong 3nm S-II (12 x 50s)

Figure 9 July 9th Imaging Results – ZS80 II ED, Bortle 5, Messier 8

IDAS 6.5nm O-III (20 x 30s)

Optolong 3nm O-III (12 x 50s)

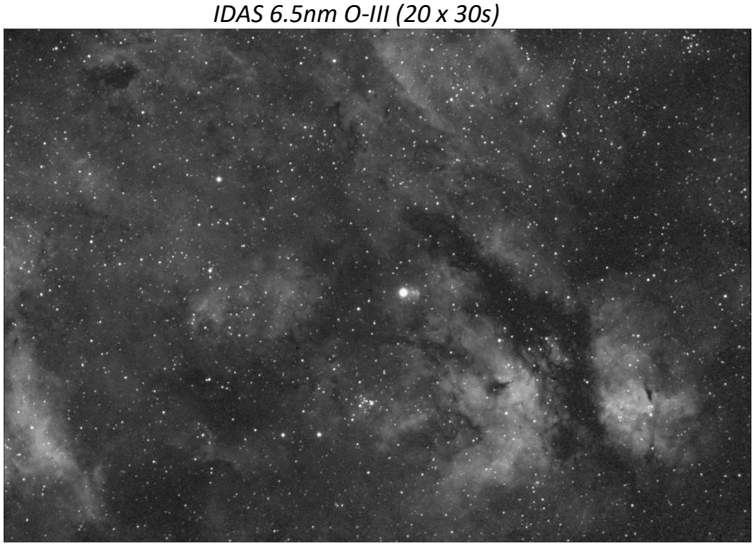

IDAS 6.8nm H-α (20x30s)

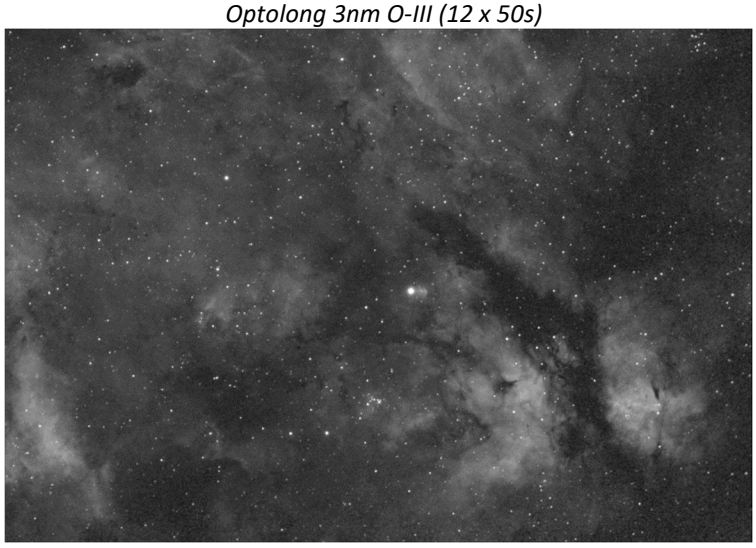

Optolong 3nm H-α (12 x 50s)

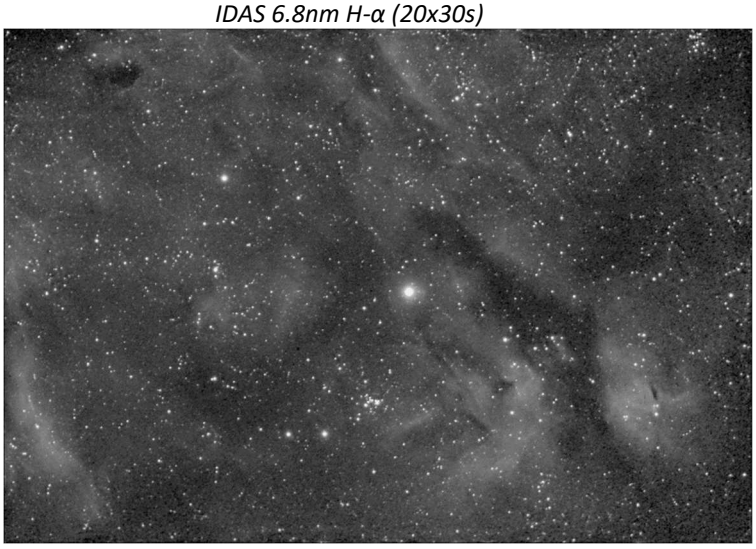

Optolong 6.5nm S-II (20 x 30s)

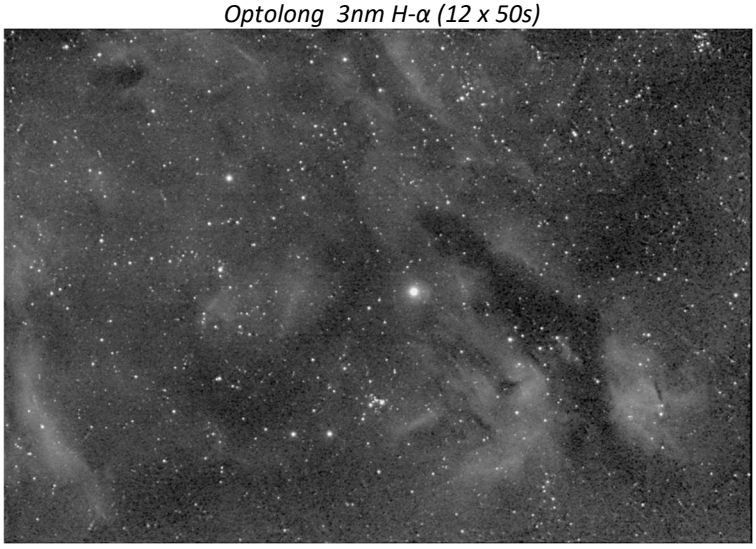

Optolong 3nm S-II (12 x 50s)

Figure 10 August 2nd Imaging Results – FMA230, Bortle 9+, IC1318

IDAS 6.5nm O-III (20 x 30s)

Optolong 3nm O-III (13 x 45s)

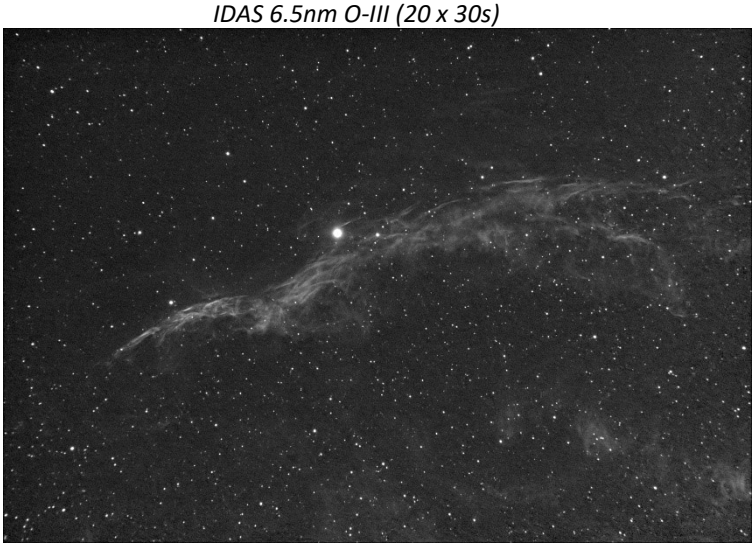

IDAS 6.8nm H-α (20x30s)

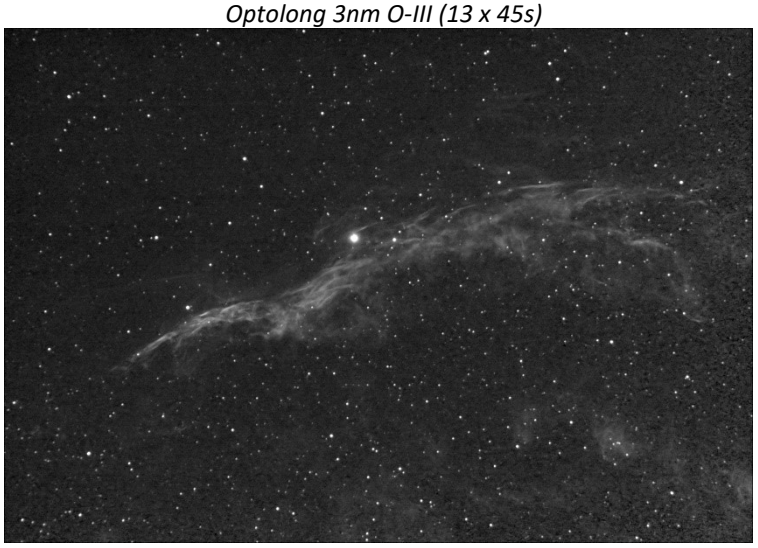

Optolong 3nm H-α (13 x 45s)

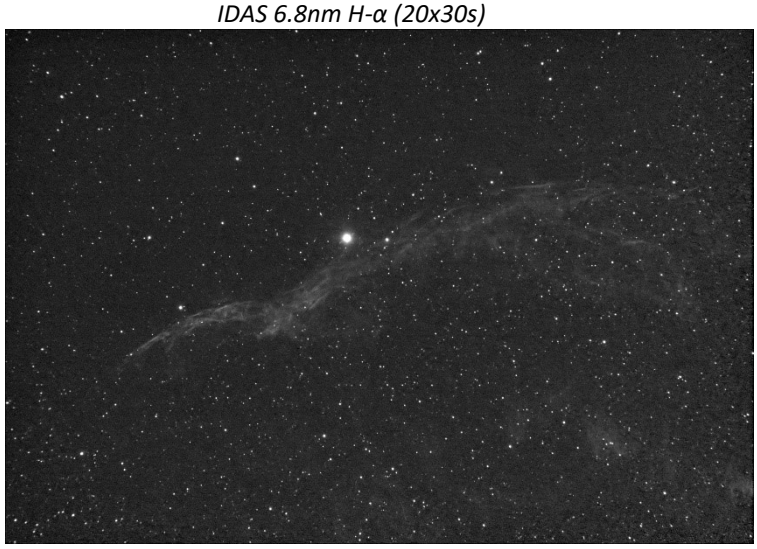

Optolong 6.5nm S-II (20 x 30s)

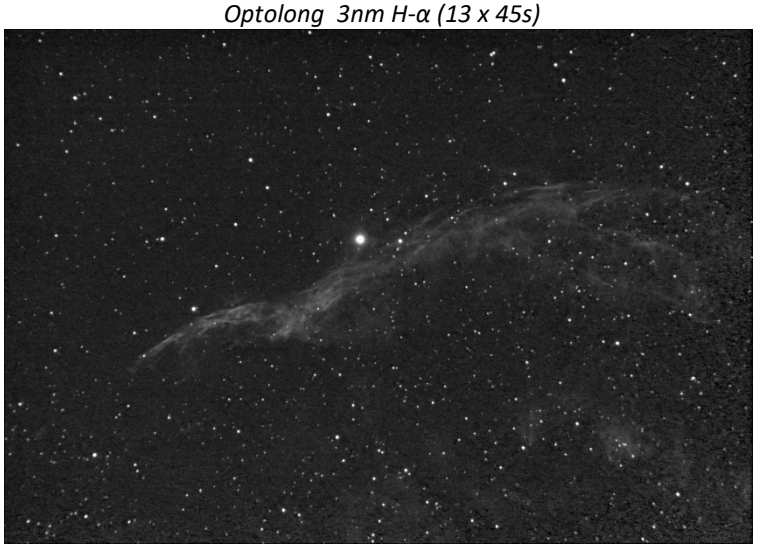

Optolong 3nm S-II (13 x 45s)

Figure 11 August 12th Imaging Results – FLT98, Bortle 9+, NGC6960

M8, 6-7nm filter set

M8, 3nm filter set

IC1318, 6-7nm filter set

IC1318, 3nm filter set

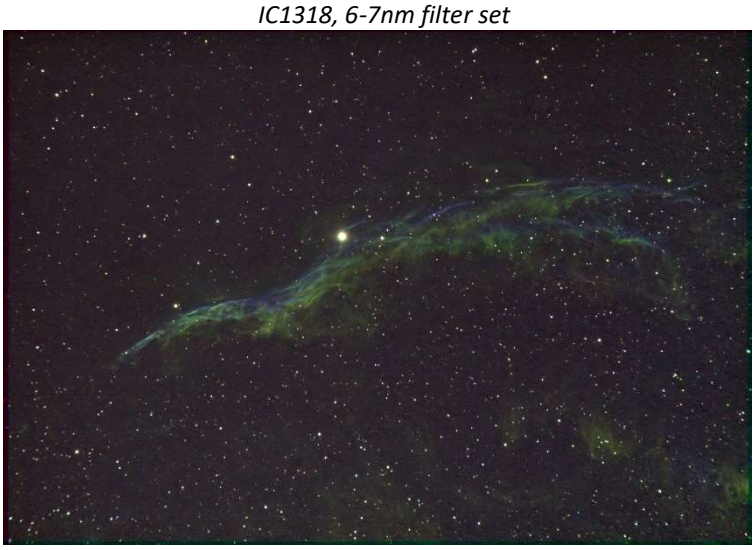

NGC6960, 6-7nm filter set

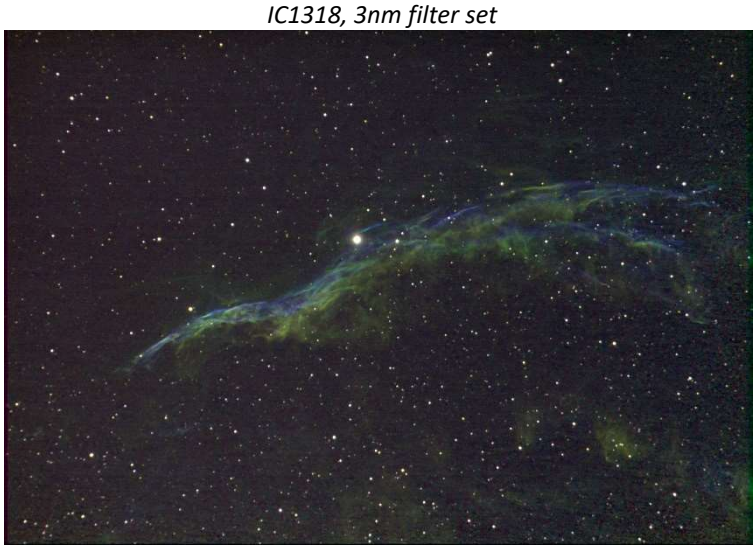

NGC6960, 3nm filter set

Figure 12 Imaging Results Combined Using Hubble Palette

Using the captured image data of M8 I was able to directly measure the contrast increase delivered by each filter, putting a number to what was already observed qualitatively from the images in Figures 9 to 12. This was accomplished by using AstroImageJ to measure the average luminance from two common areas in the images: a dark background area, and a bright nebulous area. The particular areas used are illustrated in Figure 13, with these same areas used for all the images from the various filters. Measurements of average luminance were taken from both the raw stacked images as well as a single sub-exposure. Contrast increase was calculated from the measured luminance values using the following equations:

Measured Contrast = [measured nebula luminance – measured background luminance] ÷ measured background luminance

% Contrast Increase = [contrast w/filter – contrast w/out filter] ÷ contrast w/out filter x 100

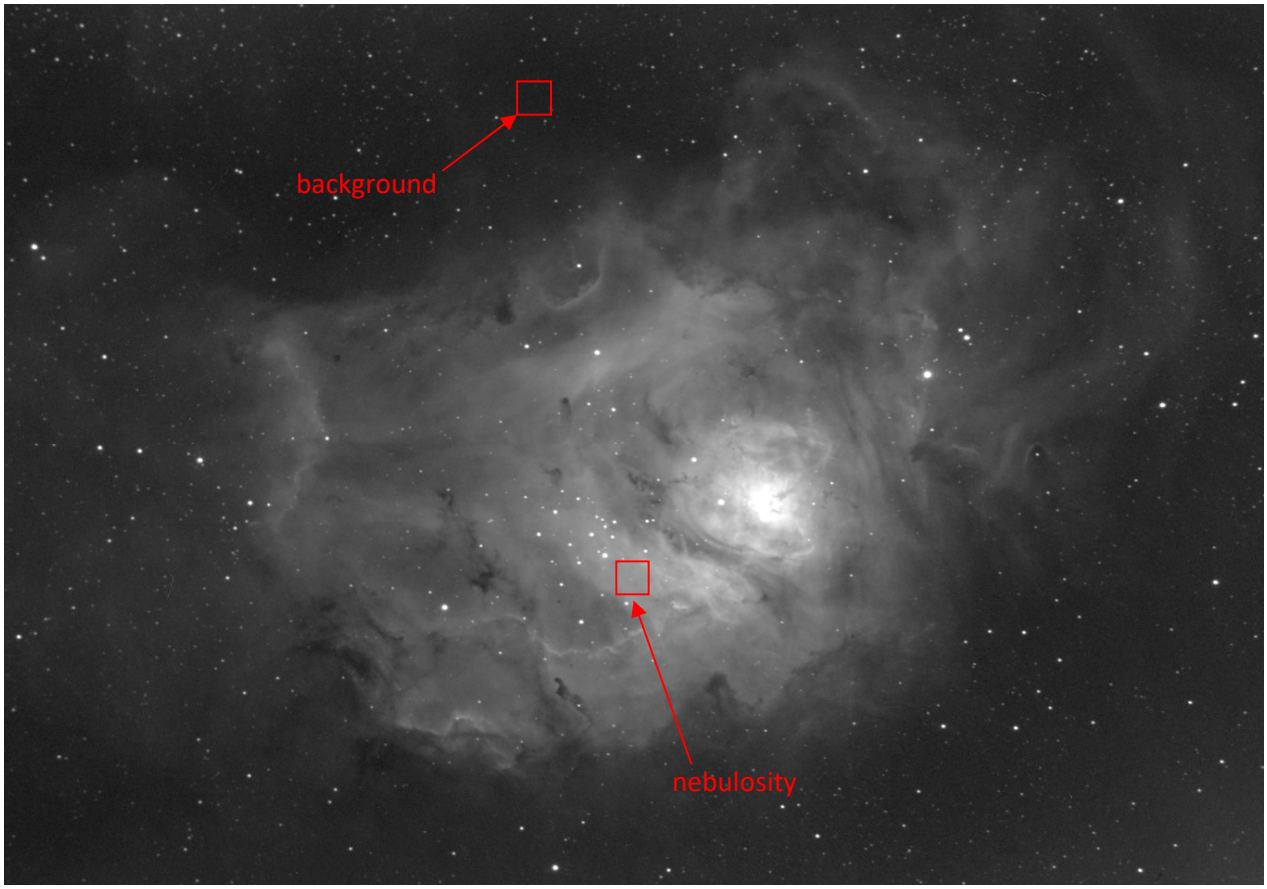

Figure 13 Areas Used for Image Analyses

The resulting contrast increase measurements are plotted in Figure 14, along with the corresponding prediction for each filter. The contrast increases measured from the H-α and O-III images were slightly lower than the predictions, most likely due to the observing conditions on the night the data was collected. The measured contrast using the two S-II filters was significantly higher than predicted. The explanation for this discrepancy probably has something to do with the sensor quantum efficiency (QE) at 672nm assumed in my calculations versus what my DS432 is actually delivering; the IMX432 sensor is much more sensitive in the deep red and infrared part of the spectrum than the IMX174 assumed in my prediction.

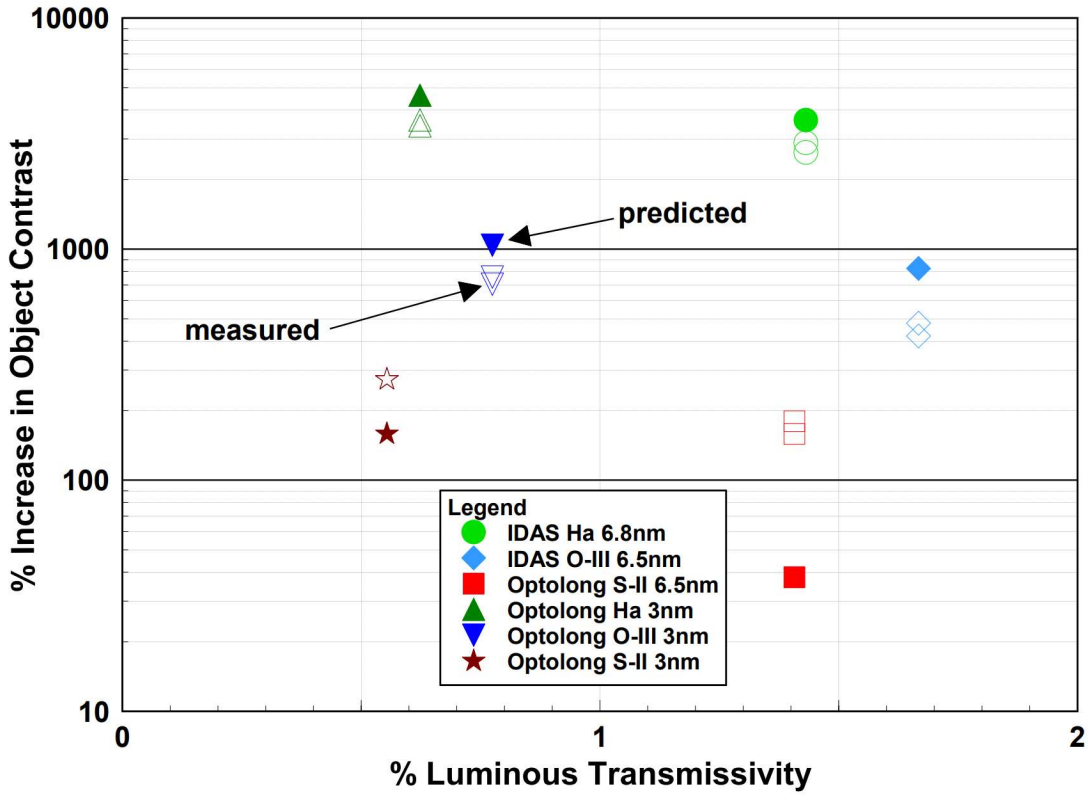

Figure 14 Measured Nebula Contrast Increase, M8 Images

The measurements of luminance from the images also allowed me to evaluate signal-to-noise ratio (SNR). When I extracted the average luminance values from each image in AstroImageJ, I also recorded the standard deviation (σ). This allowed me to calculate the SNR achieved by each filter using the following equation:

SNR = (measured nebula luminance – measured background luminance) ÷ measured nebula σ

The SNR measurement results, from single sub-exposures, are shown in Figure 15 plotted versus %LT. As expected, there is an increase in the SNR of the nebula the narrower the filter used.

Conclusions:

Based on the results of the testing described above, I have made the following conclusions:

1. Regardless of the nebula emission being captured, and the severity of your light pollution, better object contrast and SNR can be achieved by using a narrower band pass filter.
2. Although a visual comparison of the images captured during this test suggests that the improvement in performance achieved by moving to a 3nm filter set versus a 6-7nm set is very small, measurements made from the image data indicate that a real performance improvement can be achieved with 3nm filters. Whether or not, through more extensive data collection (i.e. longer sub's and more of them) and/or more rigorous post processing, the same end result can be achieved with 6-7nm filters is a question for someone with more astrophotography experience than me.

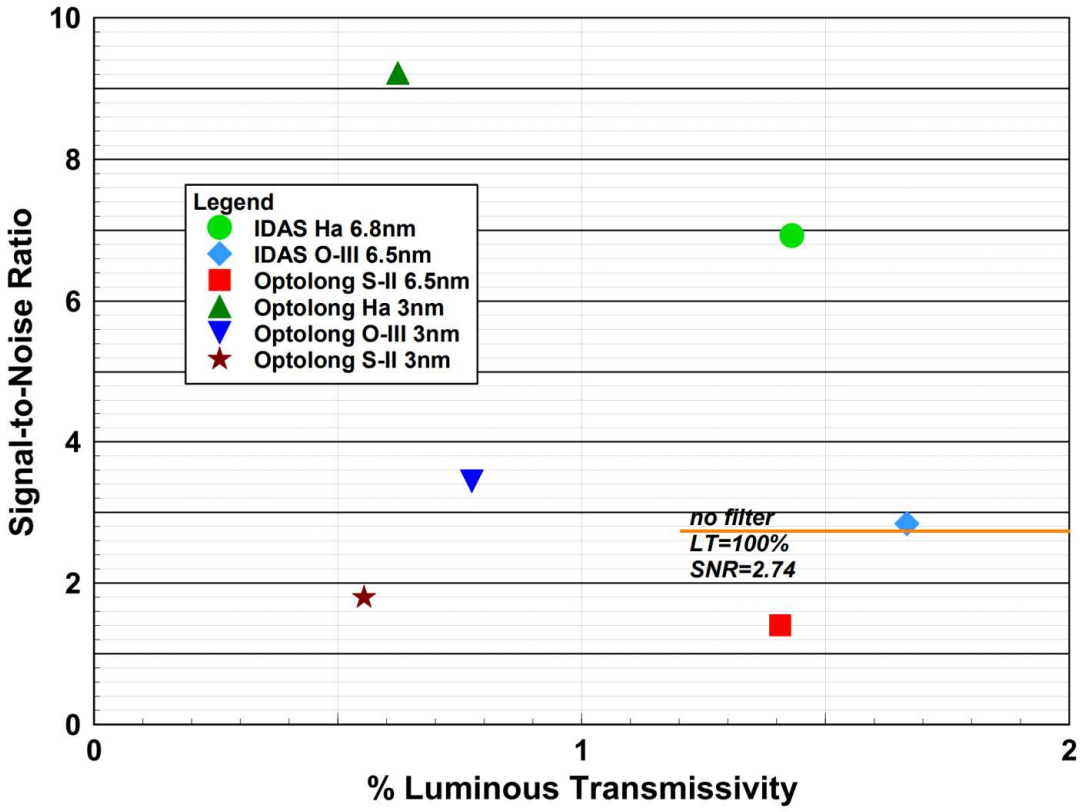

Figure 15 Measured Nebula Signal-to-Noise Ratio, Single Sub-Frame, M8 Images

3. The Optolong 3nm O-III and S-II filters performed well despite the CWL of my samples being off-band by 1.5 to 2.0nm. Presumably different samples of these filters which have their CWLs better centered will show even better performance than presented in this report.
4. In terms of cost-performance benefit, the 6-7nm filter set tested has an average SNR per $USD of 0.0040. The SNR per $USD for the 3nm set is 0.0039 at regular price and 0.0049 at the current sale price, making the sale price of the Optolong 3nm filter set a good value.
5. Any future attempts I make to use narrowband SHO filters will involve sub-exposure times longer than considered in this test (30 to 50sec). I will likely consider sub-exposure times in the 60sec range for the H-α filter, and in the 2 to 3 minute range for the O-III and S-II filters.

If you have any questions, please feel free to contact me.

Cheers!

Jim Thompson
(top-jimmy@rogers.com)